2014 IEEE/RSJ International Conference on
Intelligent Robots and Systems (IROS 2014)
September 14-18, 2014, Chicago, IL, USA

Force/vision control for robotic cutting of soft materials*

Philip Long, Wisama Khalil and Philippe Martinet*

Abstract— **In this paper, a force/vision control strategy is proposed in order to separate soft deformable materials using cooperative robots. The separation is performed by repeating a series of cuts, called passages, along a curved trajectory. The vision control is used to locally update the robot trajectory in response to both on-line deformations and off-line modeling errors. The force controller is used to ensure that the cut is performed without global deformation or damage to the surrounding area. The second robot is used to facilitate the cutting by applying external forces to the object. The control scheme is validated experimentally by cutting soft foam material.**

I. INTRODUCTION

Robotic control of deformable objects is a topic of increasing importance in the textile [1], medical [2] and food processing [3] domains. However interaction with deformable materials remains an open issue, principally due to the variability in object behavior. Several types of solutions have been proposed such as increased sensory capacity [4] or learning algorithms [5].

The meat processing industry is one of the largest potential markets for deformable object manipulation applications. A successful adaptation of robotic technology to the meat industry is illustrated in [6] resulting in improved hygiene and precision in the manufacturing environment. In [7] the reduction of the cutting force for a meat cutting robotic cell, by optimizing the cutting feed and cutting angle, is investigated. The ARMS[1] project, *A multi arms Robotic system for Muscle Separation*, aims to contribute to the robotization of the meat industry in particular the separation of beef shoulder muscles. A multi-arm system is proposed in order to deal with key challenges for example the diversity of the target object and its flexibility [8].

In this work, a force vision controller is proposed for the cutting task. In general, force control is required for contact tasks while the vision sensor is ideal for adapting to unknown environments. The combination of force and vision is achieved by either partitioning the task space into force and vision controlled directions [9], or by enforcing impedance relations between them [10], [11]. Typically, force/vision research has been focused on contour following tasks where a force is applied normal to the contour [12]. In cutting applications, this approach is no longer applicable, since in order to separate the object the tool must necessarily pass through the contour. Furthermore, the controlled force is unknown a priori and is resistive to motion rather than orthogonal. Other differences between the cutting task and the contour following case are discussed in [13].

The cutting force required is extremely difficult to predict even in tightly controlled experimental conditions as it is dependent on cutting velocity and frictional effects [14]. Intuitively, it is clear that the required cutting force can be greatly reduced if a *pressing* and *slicing* approach is performed [15]. Thus in order to cut the material, a perpendicular (pressing) motion should be combined with a transversal (slicing) motion, using either velocity control or by varying the cutting angle [16]. The cutting task can be viewed as a crack initialization/propagation problem [17] where during the crack propagation phase the effect of the *pressing* and *slicing* strategy is reduced [18]. On the other hand, in [19], the cutting action is investigated with a view to preventing soft tissue injuries that could be caused by robots.

In this paper, we propose a new control scheme which addresses the problem of robotic cutting of deformable objects. In order to cope with the unmodeled behavior external sensors, specifically force and vision sensors are considered. The force feedback is used to ensure a controlled crack propagation, leading to a precise cut. The visual feedback is used to modify the robot motion in order to follow the flexible cutting trajectory. A secondary cooperating robot is used to hold the object in place while applying a pulling force to reduce frictional effects. In terms of the cutting control, previous research have focused on optimizing cutting parameters for specific materials, whereas in this work, by using the resistive force to induce a slicing motion, this costly step can be avoided.

The paper is organized in the following way. In Section II, the robotic cell and notation are described. In Section III, the cutting strategy is explained. In Section IV the global control scheme is illustrated. In Section V the results are given. Finally, in Section VI the conclusions are drawn and future work discussed.

II. ROBOTIC CELL

Two 7-DOF Kuka LWR robots are used for this experiment, as shown in Fig.1. The cutting robot is fitted with a ATI gamma 6-axis force sensor to increase the precision of sensed cutting forces, and both a marlin 1394 camera and a razor blade are fixed to the end effector. The pulling robot is equipped with a set of hooks to grasp the soft object and uses the robot's internal torque sensors to estimate Cartesian force. The Modified Denavit-Hartenberg (MDH) notation [20] is used to describe the kinematics of the system. From these parameters, the following geometric and

*Authors are with Institut de Recherche en Communications et Cybernétique de Nantes, UMR CNRS n° 6597 1 rue de la Noë, LUNAM, École Centrale de Nantes, 44321, Nantes, France. Firstname.Lastname@irccyn.ec-nantes.fr

[1]arms.irccyn.ec-nantes.fr

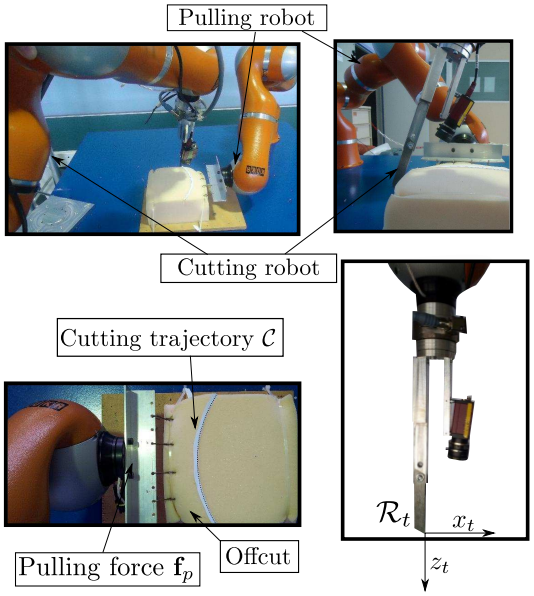

Fig. 1. Experimental Platform

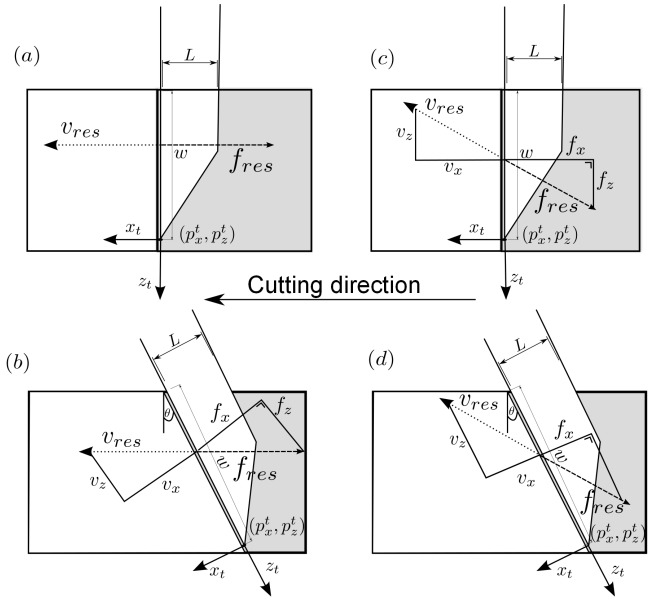

Fig. 2. Cutting Cases: (a) Cutting angle zero pure pressing, (b) Cutting angle θ pure pressing, (c) Cutting angle zero, pressing and slicing, (d) Cutting angle θ, pressing and slicing

kinematic models are obtained:

$$ {}^0\mathbf{T}_t = \begin{bmatrix} {}^0\mathbf{R}_t & {}^0\mathbf{p}_t \\ 0 & 1 \end{bmatrix} \quad , \qquad \mathbf{V}_t = {}^0\mathbf{J}_t \dot{\mathbf{q}} \tag{1} $$

The 4×4 matrix ${}^i\mathbf{T}_j$ represents the location of frame $\mathcal{R}_j$ with respect to frame $\mathcal{R}_i$ consisting of the 3×3 rotation matrix ${}^i\mathbf{R}_j$ and the 3×1 position vector ${}^i\mathbf{p}_j$. $\mathbf{J}_i$ is the kinematic Jacobian matrix of the robot evaluated at frame $\mathcal{R}_i$. $\mathbf{q}$ and $\dot{\mathbf{q}}$ are the vectors of joint positions and velocities, respectively. The subscript t indicates the tool frame.

III. Cutting Strategy

The objective of the cutting strategy is to minimize the required cutting force at the tool frame for two reasons. Firstly, if the cutting force is too large, a soft material can undergo global deformation rather than rupture, leading to the clustering of material around the cutting tool. This global deformation is undesirable from the cutting point of view since the result reduces the product quality. Secondly, a smaller cutting force reduces the energy input of the system whereas a larger cutting force may be outside the capabilities of the tool.

A. Cutting formalism

An energy balance equation (2) is used to describe the cutting process. W_r is the work done by the cutting tool. It is defined as the sum of W_c, the energy required to cut the material; W_f, the work done in overcoming the frictional effects on the blade and U, the strain energy due to global deformation of the soft material. During a pure cutting motion, it is assumed that the global deformation caused by the cutting tool is negligible, $U = 0$.

$$ W_r = W_c + W_f + U \tag{2} $$

Neglecting for the moment the frictional effects, thereby assuming the work done by the robot is used purely to cut the material, (2) becomes $W_r = W_c$. As shown in Fig.2, to cut the material the robot must move the knife along the x-axis of the tool. In order to move the tool a distance of Δx_t the robot must overcome a resistive force, denoted as ${}^t f_x$, therefore (2) is rewritten as:

$$ {}^t f_x \Delta x_t = K_c w \Delta x_t \tag{3} $$

where K_c is known as the material's fracture toughness while w is the width of the blade in contact with the material as shown in Fig.2. If a slicing motion is added, the work required to propagate the cut is now the sum of both the *pressing* and *slicing*:

$$ {}^t f_x \Delta x_t + {}^t f_z \Delta z_t = K_c w \Delta x_t \tag{4} $$

where Δz_t and ${}^t f_z$ represent the incremental displacement and force in the z_t direction, respectively. A pressing slicing ratio is defined as:

$$ \xi = \frac{\Delta z_t}{\Delta x_t} \tag{5} $$

By increasing the ratio given in (5), the resultant forces, denoted as ${}^t f_r = \sqrt{({}^t f_x^2 + {}^t f_z^2)}$, required for cutting fracture are reduced [14], [15], [18].

B. Proposed Cutting strategy

In order to minimize the required cutting forces, we propose firstly, to modify the ratio ξ in response to the presence of resistive forces and secondly, to decrease the force required to overcome the frictional effects.

It is shown in Fig.2, that the ratio ξ can be increased by either changing the cutting angle of the blade or by

increasing the velocity in the z direction. It is undesirable to increase the cutting angle during the trajectory due to both the practical difficulties and the reduction in material feed. Therefore the *slicing* velocity is linked to the resistive cutting force by an impedance controller as detailed in Section IV. In doing so, global deformations are avoided as the knife enters regions of varying material toughness. On the other hand in the absence of resistive forces, typically during the crack propagation phase, the trajectory of the cutting tool remains unchanged.

In order to reduce the effects of friction, a force denoted as $\mathbf{f}_p$ is applied by the pulling robot. The friction is due to shear as the soft material rubs against the sides of the blade. The work required to overcome the friction is defined by [15] as W_f, where

$$W_f = 2Lw\tau_f\Delta_x \tag{6}$$

where τ_f is a shear stress acting over length L. The pulling force opens the cutting valley meaning that contact between the cutting tool and the material is reduced. On the other hand this increases the deformation of the object, notably the cutting trajectory. The control law for the pulling robot is described in Section IV.

IV. Robot Controller

In order to separate the object, the cutting robot must follow a deformable trajectory on the soft body. The desired pose is updated using vision and force. The controller generates a Cartesian velocity that is transformed into a joint velocity, by firstly representing the Jacobian matrix defined in (1) in the object frame and then obtaining the pseudoinverse of this matrix, denoted as ${}^{ob}\mathbf{J}^{+}$. The joint velocity is transformed into a joint torque using the Kuka's internal controller before being sent to the motors. The pulling robot is used to both hold the object in place and to open up the cutting valley. The reference value for the pulling force is learned from experimental trials. The global control scheme is shown in Fig. 3.

A. Pulling Robot

The pulling force is applied to the object as shown in Fig.4. The pulling robot is controlled using a Cartesian stiffness strategy:

$$\boldsymbol{\tau} = {}^{0}\mathbf{J}_t^T\left(\mathbf{k}_p\ {}^{0}d\mathbf{X}_t\ + \mathbf{f}_p\right) + \mathbf{H} \tag{7}$$

$${}^{0}d\mathbf{X}_t = \begin{bmatrix} {}^{0}d\mathbf{p}_t^T & {}^{0}\delta_t^T \end{bmatrix}^T \tag{8}$$

where $\boldsymbol{\tau}$ is the commanded joint torque, ${}^{0}d\mathbf{X}_t$ contains the differential position and orientation vectors, representing the error in Cartesian space, $\mathbf{H}$ denotes the system dynamics and $\mathbf{k}_p$ is the stiffness matrix.

B. Cutting Robot

1) Trajectory Generator: The cutting robot follows a polynomial curve, $\mathcal{C}$ defined in the object frame $\mathcal{R}_{ob}$ in the form $y = a_n x^n + a_{n-1}x^{n-1} + \dots a^0$. It is important that the cutting feed, i.e. the tangential velocity, is constant. Thus the trajectory is defined in terms of the distance traveled along the curve denoted as $\mathcal{T}(t)$, where

$$\mathcal{T}(t) = r(t)D \tag{9}$$

$$D = f(x) = \int_b^a \sqrt{1 + \frac{dy^2}{dx^2}}\ dx = f(a) - f(b) \tag{10}$$

$r(t)$ is the trajectory interpolation function. D is the total curvilinear length of the polynomial curve, obtained from (10), where a and b are the extremities of the curve. For any value of $\mathcal{T}(t)$, the corresponding value of x is obtained by solving the equation $f(x) - (\mathcal{T}(t) + f(b)) = 0$.

p_x^d and p_y^d, the desired positions in the x direction and y direction, respectively, are obtained from $\mathcal{T}(t)$ and $\mathcal{C}$. In order to complete the separation, the robot must cut the material along the curve at a desired depth denoted as p_z^d. This motion is known as a passage. At time t, as shown in Fig. 4, the knife's desired location in the object frame is given as ${}^{ob}\mathbf{T}_t^d = {}^{ob}\mathbf{T}_c\ {}^{c}\mathbf{T}_t(\theta)$. In detail:

$${}^{ob}\mathbf{T}_t^d = \begin{bmatrix} \mathbf{s}^d & \mathbf{n}^d & \mathbf{a}^d & \mathbf{p}^d \\ 0 & 0 & 0 & 1 \end{bmatrix} \cdot\ {}^{c}\mathbf{T}_t(\theta) \tag{11}$$

where ${}^{c}\mathbf{T}_t(\theta)$ is used to make the trajectory consistent with the cutting angle θ. The angle θ is fixed throughout the trajectory and should be chosen to ensure the camera has a good view of the trajectory close to the knife. From Fig. 2 it can be seen that the cutting angle is defined by a rotation around the y-axis of the tool frame. $\mathbf{p}^d$ the desired position is given as:

$$\mathbf{p}^d = \begin{bmatrix} p_x^d & p_y^d & p_z^d \end{bmatrix}^T \tag{12}$$

The rotation matrix is obtained from the following vectors:

$$\mathbf{s}^d = \begin{bmatrix} \frac{1}{\sqrt{\left(1 + \frac{dy}{dx}^2\right)}}, & \frac{\frac{dy}{dx}}{\sqrt{\left(1 + \frac{dy}{dx}^2\right)}}, & 0 \end{bmatrix}^T \tag{13}$$

$$\mathbf{n}^d = \begin{bmatrix} \frac{-\frac{dy}{dx}}{\sqrt{\left(1 + \frac{dy}{dx}^2\right)}}, & \frac{1}{\sqrt{\left(1 + \frac{dy}{dx}^2\right)}}, & 0 \end{bmatrix}^T \tag{14}$$

$$\mathbf{a}^d = \begin{bmatrix} 0, & 0, & -1 \end{bmatrix}^T \tag{15}$$

As shown in Fig.4, $\mathbf{s}^d$ is the desired cutting direction, which is tangential to $\mathcal{C}$. $\mathbf{a}^d$ is the axis normal to the object's surface while $\mathbf{n}^d$ is the remaining orthogonal axis of the frame. $\frac{dy}{dx}$ is evaluated at p_x^d.

2) Force Controller: The force controller is used to ensure the material is cut cleanly i.e. no global deformation occurs. In this case an adaptive controller is defined at the tool frame to generate the force correction term ${}^{ob}d\mathbf{X}_t^f$. However in contrast to the classical case, for the cutting task the force controller is designed so that the resistive force creates a change in position in an orthogonal axis. Referring to Fig. 2, the ${}^{t}f_x$ is the resistive force of the cut, the change in position is defined as:

$$\Delta z_t = \min\begin{pmatrix} 0, & k_z\ {}^{t}f_x \end{pmatrix} \tag{16}$$

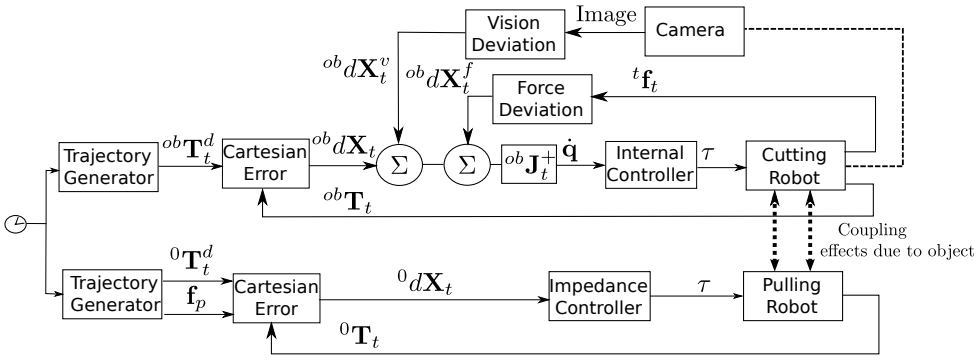

Fig. 3. Global Control Scheme

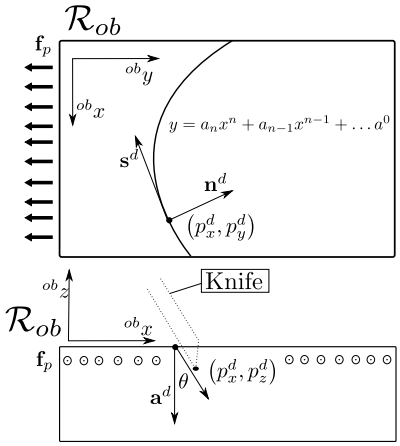

Fig. 4. Definition of desired variables

where k_z is a positive gain. From (5) and (16), it can be seen that in response to a resistive force, the velocity is increased in the z-direction, thereby increasing the *slice/press* ratio, ξ and reducing the resistive forces. This is turn allows the cutting to continue without deforming the material. By using the min function the positive values of (16) are rejected. These values are due to noisy force sensor measurements and would cause the knife to enter deeper into the material.

3) Vision Controller: The vision controller updates the trajectory of the knife in response to on-line deformations by creating a deviation, denoted as $^{ob}d\mathbf{X}_t^v$ as follows:

1) The vision system extracts the image coordinates of (u_i, v_i), (u_j, v_j) and (u_k, v_k), a series of points ahead of the image projection of tool point
2) The normalized position of a point i is reconstructed using the intrinsic camera parameters, $\mathbf{A}$, which relate the image coordinates to the coordinates in the perspective plane:

$$\begin{bmatrix} \frac{p_{xi}^v}{p_{zi}^v} \\ \frac{p_{yi}^v}{p_{zi}^v} \\ 1 \end{bmatrix} = \mathbf{A} \begin{bmatrix} u_i \\ v_i \\ 1 \end{bmatrix} \tag{17}$$

3) The depth of a point, p_{zi}^v, is estimated using the material height and the tool position, the depth estimation allows the reconstruction of the 3D position of the point
4) Since the camera gives a local view of the trajectory, the curvature within this window is quite small and can be approxiamted by a straight line. By fitting this line to the Cartesian position of points i, j and k the vectors $\mathbf{s}$ and then $\mathbf{n}$ are obtained
5) From step 3 and step 4 the desired matrix given by vision $^{ob}\mathbf{T}_i^v$ at a point i can be written

In order to generate an error vector, the curve $\mathcal{C}$ is evaluated at p_{xi} allowing a desired matrix $^{ob}\mathbf{T}_i^d$ to be obtained. This in turn is used to calculate the vision generated deviation which acts in one translational direction and three rotational directions:

$$\Delta p_{yi} = p_{yi}^d - p_{yi}^v \tag{18}$$

$$\Delta^{ob}\mathbf{R}_i = {}^{ob}\mathbf{R}_i^d \left({}^{ob}\mathbf{R}_i^v\right)^T \tag{19}$$

V. Experimental Validation

In this section the cutting experiment is described. The robot cuts the material until the resistive force grows in magnitude and a slicing phase is performed. If the cutting tool frame reaches a greater height than the object, the robot returns to the initial position to restart the passage.

A. Experimental Setup

The experimental setup is shown in Fig.1. A 200mm $\times$ 200mm $\times$ 100mm block of foam known as Bultex © is used. A series of dots, serving as the visual markers, are attached to the foam. The cutting trajectory is shifted from these dots by a small distance to ensure the knife does not cut the visual marker.

B. Results

Each passage allows the robot to cut further and further along the trajectory. This gradual progression is seen in Fig.5, Fig.6 and Fig.7.

In Fig.5, the off-line estimation of the curve, the visually extracted curve and the robot position are shown. This graph shows that the desired trajectory is deformed due to the force

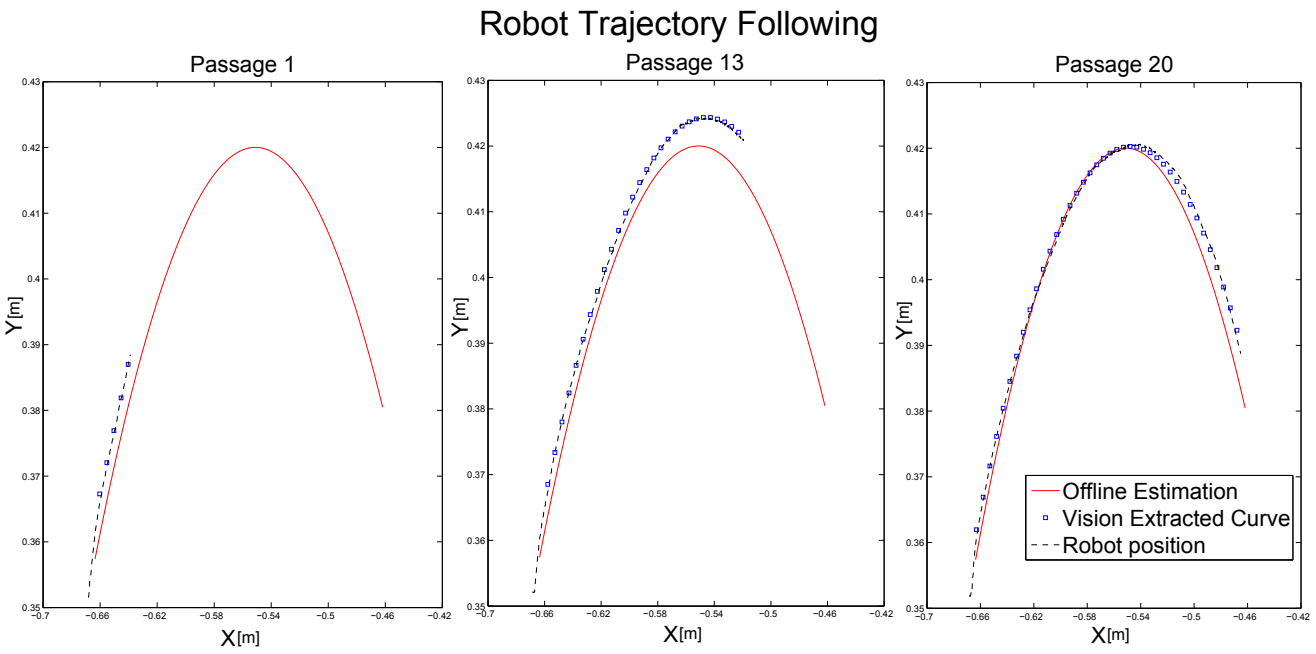

Fig. 5. Displacement in the x-y plane of the object

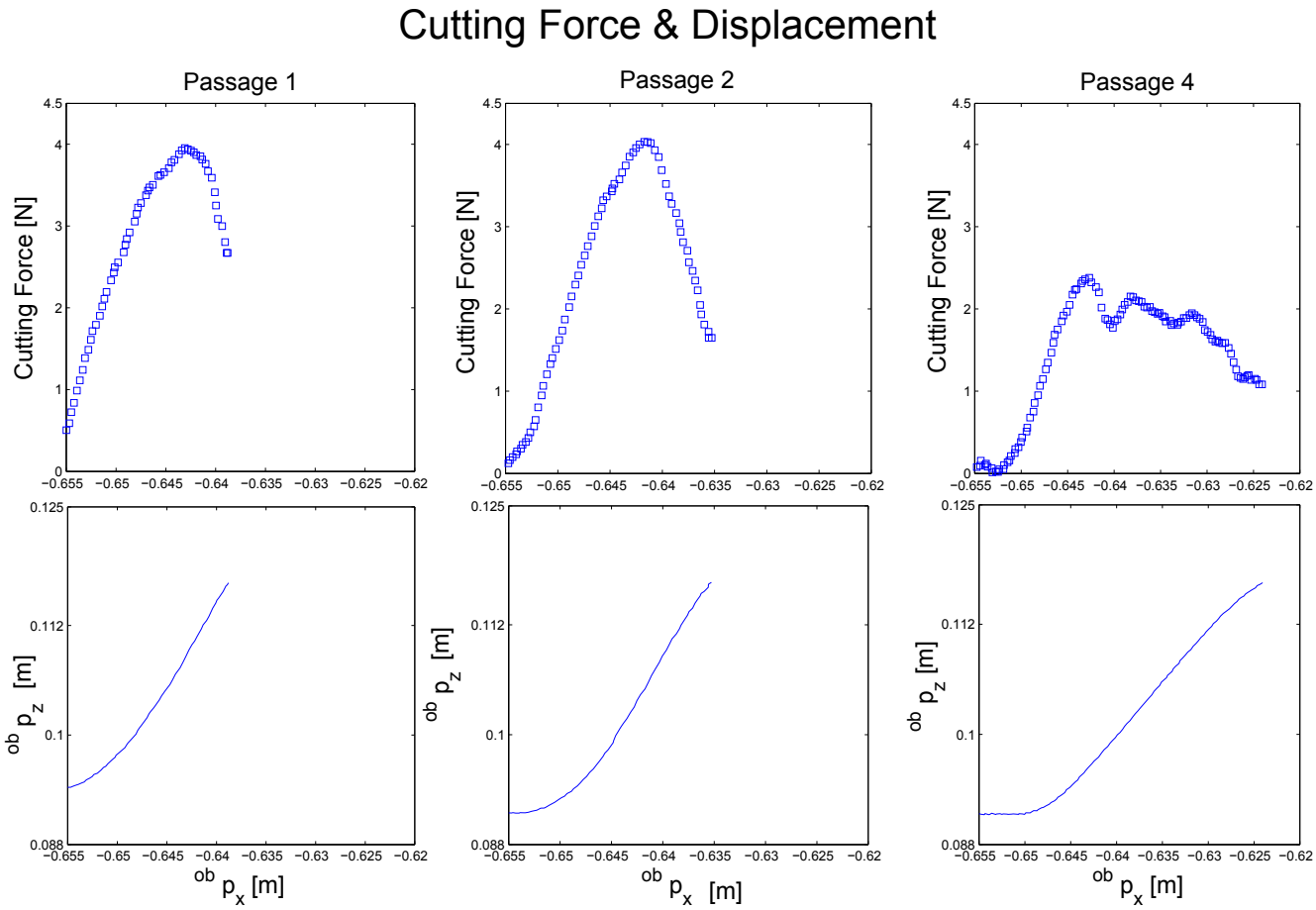

Fig. 6. Cutting force and the displacement along the x and z axes during the initial cutting phase

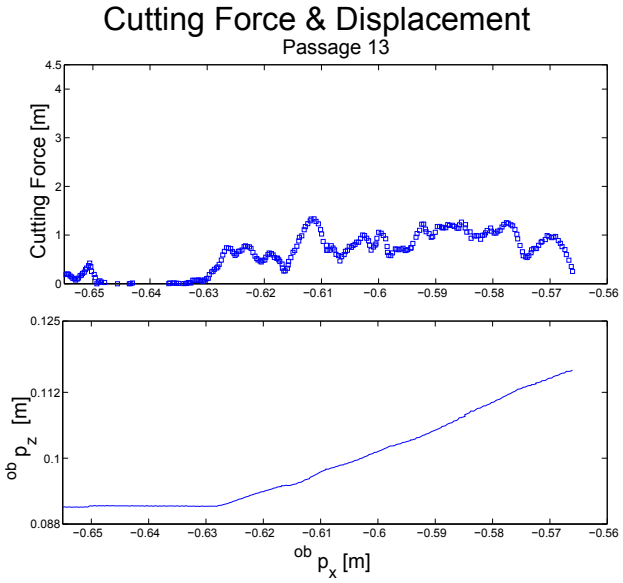

Fig. 7. Forces and Displacement during the cutting propagation phase

applied by the pulling robot. The vision controller allows the robot to cut along the new trajectory. In Fig.5, Passage 20 shows that the cutting trajectory begins to resemble the initial estimation as the separation reaches its end. This is expected since $\mathbf{f}_p$ at this moment is applied to the offcut. Therefore as the cutting proceeds, the deformation effect due to $\mathbf{f}_p$ on the main part of the object is reduced, meaning the cutting trajectory returns to its original undeformed shape.

Fig.6 and Fig.7 show the cutting force in the tool frame and the z position of the tool frame versus the progress along the curve during the crack initialization and propagation phase, respectively. In Fig.6 the increase in the resistive cutting force causes the controller to create a slicing action which in turn results in a decrease of the force. During the crack propagation phase in Fig.7, the magnitude of the resistive force has decreased. Finally in Fig.7, for the phases where cutting has taken place, the sensed force is close to zero showing the absence of frictional forces due to the pulling robot.

VI. Conclusions

In this paper, a force/vision controller is proposed and validated for the separation of deformable objects. A force controller is designed so that the increase in the resistive force generates a slicing motion thus avoiding any rupture or global deformation of the object. The vision controller is used to modify on-line the robot trajectory.

Future work will focus on the validation of this scheme for meat cutting applications, including the integration of a third robot to visually track the deformable object and act as a global supervisor. Furthermore a model of the deformable object will be added to the control loop, this model will allow the on-line calculation of the pulling force.

ACKNOWLEDGMENT

This paper describes work carried out in the framework of the ARMS project, a project funded by the ANR (Agence Nationale de la Recherche), reference ANR-10-SEGI-000. Parts of the equipment used here were funded by the project ROBOTEX, reference ANR-10-EQPX-44-01.

References

[1] M. Saadat and P. Nan, "Industrial applications of automatic manipulation of flexible materials," *Industrial Robot: An International Journal*, vol. 29, no. 5, pp. 434–442, 2002.

[2] K. Cleary and C. Nguyen, "State of the art in surgical robotics: clinical applications and technology challenges," *Computer Aided Surgery*, vol. 6, no. 6, pp. 312–328, 2001.

[3] R. J. M. Masey, J. O. Gray, T. J. Dodd, and D. G. Caldwell, "Guidelines for the design of low-cost robots for the food industry," *Industrial Robot: An International Journal*, vol. 37, no. 6, pp. 509–517, 2010.

[4] D. Navarro-Alarcón, Y.-H. Liu, J. G. Romero, and P. Li, "Model-free visually servoed deformation control of elastic objects by robot manipulators," *IEEE Transactions on Robotics and Automation*, vol. 29, pp. 1457–1468, dec 2013.

[5] B. Balaguer and S. Carpin, "Combining imitation and reinforcement learning to fold deformable planar objects," in *2011 IEEE/RSJ International Conference on Intelligent Robots and Systems (IROS)*, pp. 1405–1412, IEEE, 2011.

[6] L. Hinrichsen, "Manufacturing technology in the danish pig slaughter industry," *Meat science*, vol. 84, no. 2, pp. 271–275, 2010.

[7] G. Guire, L. Sabourin, G. Gogu, and E. Lemoine, "Robotic cell for beef carcass primal cutting and pork ham boning in meat industry," *Industrial Robot: An International Journal*, vol. 37, no. 6, pp. 532–541, 2010.

[8] P. Long, W. Khalil, and P. Martinet, "Modeling and control of a meat-cutting robotic cell," in *2013 15th International Conference on Advanced Robotics (ICAR)*, pp. 61–66, IEEE, 2013.

[9] D. Xiao, B. Ghosh, N. Xi, and T. Tarn, "Sensor-based hybrid position/force control of a robot manipulator in an uncalibrated environment," *IEEE Transactions on Control Systems Technology*, vol. 8, no. 4, pp. 635–645, 2000.

[10] V. Lippiello, B. Siciliano, and L. Villani, "Robot interaction control using force and vision," in *Intelligent Robots and Systems, 2006 IEEE/RSJ International Conference on*, pp. 1470–1475, IEEE, 2006.

[11] Y. Mezouar, M. Prats, and P. Martinet, "External hybrid vision/force control," in *Intl. Conference on Advanced Robotics (ICAR07)*, 2007.

[12] J. Baeten, W. Verdonck, H. Bruyninckx, and J. De Schutter, "Combining force control and visual servoing for planar contour following," *Int. J. of Machine Intelligence and Robotic Control*, vol. 2, no. 2, pp. 69–75, 2000.

[13] G. Zeng and A. Hemami, "An adaptive control strategy for robotic cutting," in *Proceedings of 1997 IEEE International Conference on Robotics and Automation*, vol. 1, pp. 22–27, IEEE, 1997.

[14] D. Zhou, M. R. Claffee, K.-M. Lee, and G. V. McMurray, "Cutting,'by pressing and slicing', applied to the robotic cut of bio-materials. ii. force during slicing and pressing cuts," in *Proceedings of 2006 IEEE International Conference on Robotics and Automation*, pp. 2256–2261, IEEE, 2006.

[15] A. Atkins, X. Xu, and G. Jeronimidis, "Cutting, by pressing and slicing,of thin floppy slices of materials illustrated by experiments on cheddar cheese and salami," *Journal of Materials Science*, vol. 39, no. 8, pp. 2761–2766, 2004.

[16] G. Arnold, L. Leiteritz, S. Zahn, and H. Rohm, "Ultrasonic cutting of cheese: Composition affects cutting work reduction and energy demand," *International Dairy Journal*, vol. 19, no. 5, pp. 314–320, 2009.

[17] M. Mahvash and V. Hayward, "Haptic rendering of cutting: A fracture mechanics approach," *Haptics-e*, vol. 2, no. 3, pp. 1–12, 2001.

[18] E. Reyssat, T. Tallinen, M. Le Merrer, and L. Mahadevan, "Slicing softly with shear," *Physical review letters*, vol. 109, no. 24, p. 244301, 2012.

[19] S. Haddadin, A. Albu-Schaffer, F. Haddadin, J. Rosmann, and G. Hirzinger, "Study on soft-tissue injury in robotics," *Robotics & Automation Magazine, IEEE*, vol. 18, no. 4, pp. 20–34, 2011.

[20] W. Khalil and J. Kleinfinger, "A new geometric notation for open and closed-loop robots," in *Proceedings. 1986 IEEE International Conference on Robotics and Automation*, vol. 3, pp. 1174–1179, IEEE, 1986.